



Published in final edited form as:

Abdom Radiol (NY). 2018 July ; 43(7): 1627–1633. doi:10.1007/s00261-017-1339-5.

Evaluation of an Abbreviated Screening MRI Protocol for Patients at Risk for Hepatocellular Carcinoma

Jennifer Y. Lee¹, Eugene J. Huo¹, Stefanie Weinstein^{1,4}, Charmaine Santos⁴, Alexander Monto^{2,5}, Carlos U. Corvera³, Judy Yee^{1,4}, Thomas A. Hope^{1,4}

¹Department of Radiology and Biomedical Imaging, University of California, San Francisco, CA

²Department of Gastroenterology, University of California, San Francisco, CA

³Department of Surgery, University of California, San Francisco, CA

⁴Department of Radiology, Veterans Affairs Medical Center, San Francisco, CA

⁵Department of Medicine, Veterans Affairs Medical Center, San Francisco, CA

Abstract

Purpose: In this study, we compare an abbreviated screening MRI protocol (aMRI), utilizing only dynamic contrast-enhanced images, to a conventional liver MRI (cMRI) for the characterization of observations in at-risk patients.

Materials & Methods: 164 consecutive HCC screening MRIs were retrospectively analyzed. Two sets of deidentified image sets were created: one with all acquired sequences including T2- and diffusion-weighted sequences (cMRI), and one with only T1-weighted precontrast and dynamic post-contrast images utilizing an extracellular gadolinium contrast agent (aMRI). Three readers assigned a LI-RADS score based on the lesion with the highest LI-RADS category using the aMRI and cMRI data sets during separate reads.

Results: There was no change between the aMRI and cMRI LI-RADS categorization in 93%, 96% and 96% of cases for readers 1, 2 and 3 respectively. In the majority of the discrepant cases, the score increased from LI-RADS 3 to LI-RADS 4 due to the presence of ancillary features on T2 and DWI. Kappa values for interobserver variability demonstrated fair to moderate LI-RADS agreement among the 3 readers.

Conclusion: There was strong agreement between the abbreviated T1-only MRI protocol and a full liver MRI, with only 5% of cases changing LI-RADS categorization due to the inclusion of T2 and DWI. The estimated time to run this abbreviated MRI is approximately 7–10 minutes, possibly allowing for a more cost-effective screening MRI than our cMRIs.

Correspondence to: Thomas A. Hope; thomas.hope@ucsf.edu.

Conflict of interest: Jennifer Y. Lee, Eugene J. Huo, Stefanie Weinstein, Charmaine Santos, Alexander Monto, Carlos U. Corvera, Judy Yee and Thomas A. Hope declare that they have no conflict of interest.

Ethical approval: All procedures performed in studies involving human participants were in accordance with the ethical standards of the institutional and/or national research committee and with the 1964 Helsinki declaration and its later amendments or comparable ethical standards.

Informed consent: The need for individual informed consent was waived by our institutional review board (IRB) for this retrospective study.

Keywords

hepatocellular carcinoma; MRI; screening; LI-RADS

INTRODUCTION

Hepatocellular carcinoma (HCC) is the most common primary malignancy of the liver and a common cause of death from cancer worldwide (1). Although there have been significant advancements in medical, percutaneous and surgical therapy (including liver transplantation) for HCC in recent years, all management and treatments rely on accurate diagnosis and staging of liver lesions by noninvasive cross-sectional imaging. Despite significantly higher sensitivity and specificity of computed tomography (CT) and magnetic resonance imaging (MRI) ultrasound (US) is currently the preferred modality of HCC screening in at-risk patients, largely due to cost (2–4).

The Liver Imaging Reporting and Data System (LI-RADS), introduced by the ACR in 2011 and subsequently updated in 2013 and 2014, is designed to standardize radiologic diagnosis of HCC, allow for consistent terminology and reduce variability in reporting as well as enhance communication with referring physicians (5,6). Five major criteria are used in assigning the LI-RADS category to a liver lesion/observation: size, arterial phase hyperenhancement, washout appearance, capsule appearance and threshold growth. Multiple ancillary features, including T2 hyperintensity and diffusion restriction, can be used to upgrade the LI-RADS category but cannot upgrade a lesion to a LI-RADS 5 category.

US without contrast cannot be used to provide a LI-RADS categorization; therefore, if cost were not an issue, CT and MRI may be preferred to US for screening. If a screening MRI could be performed in a shorter period of time, it may be possible to decrease the cost of performing an MRI to be competitive with US. Although currently there are no billing codes for abbreviated MRIs, a shorter screening MRI would allow for more patients to be imaged in the same period of time. Additionally, MRI does not utilize ionizing radiation, which also may be a benefit over CT. Therefore, in this study, we compare an abbreviated screening MRI protocol (aMRI), utilizing only dynamic contrast-enhanced images, to conventional liver MRI (cMRI) in detection and LI-RADS categorization of liver observations in a screening population.

MATERIALS AND METHODS

Patients

The local institutional review board approved this HIPAA-compliant retrospective study, and informed consent was waived. One hundred sixty-four consecutive patients at increased risk for hepatocellular carcinoma underwent magnetic resonance imaging at our institution, a Veteran's Affairs hospital, over a two-year period from March 2014 to March 2016. Demographic and clinical information was obtained from the electronic medical record, and cirrhosis was documented based on either percutaneous biopsy or imaging results. Patients with a known HCC or history of HCC treated with embolization therapy were excluded.

Patients with prior HCC that was treated with curative therapy (surgical resection, radiofrequency ablation, microwave ablation and/or liver transplant) were included if the immediate prior study demonstrated no evidence of HCC. After preliminary analysis, an additional 8 cases were excluded due to severe motion artifact and/or other technical factors related to the scan.

MR imaging techniques

All images were obtained on a 3.0T MRI system (Skyra, Siemens Healthcare; Erlangen, Germany), using a 32-channel phased-array coil. In each patient, 0.1 mmol/kg of gadobutrol (Gadavist®; Bayer HealthCare, Whippany, NJ) was injected at a rate of 2 mL per second, followed by a 20-mL saline flush. A 1 mL bolus of intravenous contrast was used as a timing bolus. In addition to localizers, the following sequences were obtained:

1. Coronal T2-weighted single-shot turbo spin-echo (HASTE) with the following parameters: matrix size 256×230 , flip angle 180° , TR/TE of 1400/87 ms, and 5 mm slice thickness with a 1 mm gap.
2. Axial T2 HASTE with fat saturation using spectrally adiabatic inversion recovery (SPAIR) and 320×219 matrix, 160° flip angle, TR/TE of 1600/95, parallel imaging factor of 2, and 5 mm slice thickness with a 1 mm gap.
3. Diffusion-weighted imaging with 128×112 matrix, 2604 Hz bandwidth, TR/TE 1920/55 ms, GRAPPA parallel imaging acceleration factor of 2, and 6 mm slice thickness with 1.2 mm gaps. Three b-values were used, $b = 0, 50$ and 700 s/mm^2 , with 2, 2 and 6 signal averages for each b-value, respectively. Respiratory navigators were used.
4. Precontrast axial T1-weighted in- and out-of-phase (DIXON) with the following parameters: 320×181 matrix, 9.0° flip angle, opposed-phase TR/TE 4.1/1.33, in-phase TR/TE 4.1/2.56, and 3.2 mm slice thickness.
5. Precontrast axial T1-weighted spoiled gradient echo (VIBE: volumetric interpolated breath-hold examination) (7), with spectral fat saturation and 288×169 matrix, 450 kHz bandwidth, 9.0° flip angle, TR/TE 3.83/1.85, and 3.0 mm slice thickness.
6. Triple arterial-phase imaging: performed using three sequential 8-second acquisitions in a single breath-hold (8), using a two-dimensional parallel acceleration technique (CAIPIRINHA, controlled aliasing in parallel imaging results in higher acceleration) and the same parameters as the precontrast VIBE sequence.
7. Portal venous phase and delayed phase axial VIBEs with TR/TE of 4.47/2.46 and 4.3/1.84, respectively; otherwise identical to the preceding sequences.
8. Coronal venous/delayed VIBE with 320×240 matrix, TR/TE 4.0/1.74, and 3.0 mm slice thickness.

Reading protocols and image interpretation

Two sets of de-identified reading protocols were created in OsiriX (9), one with all the sequences obtained in the original scan (cMRI), and one with only T1-weighted pre- and post-contrast sequences (aMRI). Three fellowship-trained abdominal radiologists (JL, EH and SW with 5, 12 and 15 years, respectively, of radiology experience) independently interpreted the two sets of reading protocols using OsiriX and recorded any liver observations that were present as well as their sizes (single longest axial dimension). All readers were blinded to the patients' clinical information and MRI reports. Each patient/case was assigned a LI-RADS score based on the lesion with the highest LI-RADS category, first using only the T1-weighted pre- and post-contrast sequences (aMRI). Specific imaging features were noted for each case including arterial phase hyperenhancement, washout and capsule appearance as defined by the LI-RADS v2014 guidelines (5). Separately, the same cases were categorized using all obtained sequences (cMRI), and the presence or absence of ancillary features such as T2 hyperintensity and diffusion restriction was also recorded. The two sets of reading protocols (aMRI and cMRI) were interpreted at different times to reduce recall bias.

Statistical analysis

Cohen's κ statistics were used to assess inter-reader agreement for major diagnostic features of HCC (arterial phase hyperenhancement, washout and capsule appearance) in both abbreviated MRI (dynamic contrast enhancement only) and complete MRI sequences (including T2- and diffusion-weighted images); 0–0.2 indicated slight agreement; 0.21–0.4, fair agreement; 0.41–0.6, moderate agreement; 0.61–0.8, substantial agreement and 0.81–1.00, almost perfect agreement (10). Calculations and analyses were performed using R 3.2.5 (The R Foundation for Statistical Computing, Vienna, Austria) and Excel 14.6.4 (Microsoft, Redmond, WA). A p -value of <0.05 was used to determine significance for all tests.

RESULTS

156 patients were included for analysis included 5 women and 151 men (Table 1), and the LI-RADS scores assigned by each reader are shown in Table 2. Of the 59 lesions/ observations identified, 14 lesions (24%) were less than 1.0 cm in greatest axial dimension, 27 lesions (46%) were 1.0–1.9 cm in size, and 18 lesions (31%) were 2.0 cm or larger.

For reader 1, there was no change in the LI-RADS score between aMRI and cMRI for 145 cases, and the LI-RADS score changed in 11 cases. Reader 2 found no change in the LI-RADS score for 149 cases and an increase in the LI-RADS score in 7 cases. Reader 3 found no change in the LI-RADS score for 150 cases, an increase in the LI-RADS score in 4 cases and decrease in the LI-RADS score for 2 cases. In many of the discrepant cases (8/11 for the first reader, 4/7 for the second reader and 3/6 for the third reader), the score increased from LI-RADS 3 to LI-RADS 4 due to the presence of ancillary features, most commonly T2 hyperintensity. Figure 1 shows an HCC lesion categorized as LI-RADS 5 by all 3 readers on aMRI. In Figure 2, an observation categorized as LI-RADS 3 based on aMRI alone was upgraded to LI-RADS 4 by all three readers due to the presence of ancillary features.

Calculations of inter-reader agreement for overall LI-RADS categorization (Table 3) demonstrated fair agreement for individual LI-RADS categories with κ values of 0.305 for aMRI and 0.308 for cMRI. When LI-RADS 1 and LI-RADS 2 were combined and compared against LI-RADS 3, 4 and 5 combined (Figure 3), there was moderate agreement between the three readers with κ of 0.508 and 0.489 for aMRI and cMRI, respectively). Inter-reader agreement of individual imaging features showed κ of 0.354 for arterial phase hyperenhancement, 0.355 for washout and 0.416 for capsule.

DISCUSSION

In this study, we found a small difference in the LI-RADS categorization of liver observations between the aMRI and cMRI reading protocols. Of the low percentage (approximately 5%) of LI-RADS scores that changed between aMRI and cMRI, the majority were LI-RADS 3 lesions that were upgraded to LI-RADS 4 due to the presence of ancillary features such as T2 hyperintensity and diffusion restriction.

Although MRI has been demonstrated to be superior to both US and CT in screening and characterization of hepatocellular carcinoma (3,11), it remains underutilized in HCC screening largely due to concerns about cost (2). One contributing factor is amount of time it takes to perform a routine or cMRI at most institutions, which generally include time-intensive sequences such as fat-saturated T2- and high-b-value diffusion-weighted sequences, in addition to the pre- and dynamic post-contrast T1-weighted images needed for reliable detection and characterization of liver lesions/observations.

A typical liver MRI may take 30–40 minutes, and possibly longer if a hepatocellular contrast agent is utilized. However, with an abbreviated MRI that includes only localizer images followed by pre- and dynamic post-contrast T1-weighted sequences using an extracellular gadolinium contrast agent, one would obtain all the information needed to detect liver lesions and assign appropriate LI-RADS categories, essentially equivalent to a multiphase liver CT. An aMRI examination would likely only take 7–10 minutes to complete, similar to CT, though MRI is more sensitive for HCC than CT especially when multiple arterial phases are acquired (11,12). It is possible that an aMRI could be faster to perform than a US that generally takes at least 30 minutes to complete, including the time spent by the sonographer reviewing images with the supervising radiologist. Ultrasound, in addition to being very operator-dependent, is much less sensitive than both CT and cMRI for hepatic lesions, particularly in cirrhotic livers and in the posterior right hepatic lobe due to increased sound attenuation of diseased liver parenchyma, among other technical limitations (3,13).

There was seemingly high variability in LI-RADS scores among the three readers as demonstrated by fair to moderate κ values, which may be partly due to the low incidence of lesions and, therefore, imaging features such as arterial phase hyperenhancement, in this screening population. A recent study by Ehman et al. demonstrated κ scores of 0.4 for arterial phase hyperenhancement, 0.56 for washout and 0.11 for capsule (14), which is not significantly different from the κ scores obtained in this study. Other studies have also shown substantial interobserver inconsistency for individual imaging characteristics of HCC, particularly ancillary features (15). This variability may be related to differences in

experience level, interpretation of more subjective ancillary features such as nodule-in-nodule appearance (5). Additionally, in our study readers had to select the lesion with the highest LI-RADS category, while in previous studies the lesion was preselected adding an extra level of disagreement. Another reason for the variability was that many of the observed lesions in our screening population were small (nearly 75% less than 2 cm in greatest axial dimension), limiting evaluation of specific imaging and ancillary features.

One could argue that this high degree of inter-reader variability, in contrast to the relatively low percentage of LI-RADS categorization discrepancies between aMRI and cMRI, provides further support for the clinical equivalence of these two protocols. Therefore, the increased sensitivity and specificity of MRI in detection of liver lesions compared to US as demonstrated in multiple studies can be applied to aMRI (2,3,11,13).

Currently in the US, there is no mechanism in place to charge a lower rate for an aMRI compared to cMRI. Nonetheless, in many healthcare systems in the US where care is provided through bundled costs or in a vertically integrated system such as Kaiser or the Veterans Health system, an approach using aMRI may be implemented. By decreasing the amount of time for an imaging study, more aMRIs could be performed per unit time, and therefore there may be an associated increase in the access to MRI that may be limiting current usage of MRI for HCC screening. Our results do suggest that a further study should be performed to test the reproducibility, time and cost savings associated with the aMRI protocol in order to determine if aMRI may be an appropriate screening test for patients at risk for HCC.

This study had several limitations. First, our study was performed at 3.0T, and so our results may not be translatable to 1.5T magnets. Second, our aMRI protocol was designed for screening purposes, we excluded patients with current viable HCC and/or HCC treated by embolization therapy, which accounts for a significant portion of liver MRIs performed in daily practice and these studies may still require a complete MRI study. In addition, we simulated an abbreviated MRI rather than actually performing one; therefore, the true length of the examination is uncertain. While the estimated time to run an aMRI is approximately 7–10 minutes, this does not account for the time needed to place a peripheral IV as well as the scanner turnaround time that includes getting the patient on and off the table.

CONCLUSION

There was only a small difference in detection and characterization of liver lesions between our abbreviated T1-only MRI protocol and a complete liver MRI, with 5% of cases changing LI-RADS categorization due to the inclusion of T2 and DWI. The estimated time to run this abbreviated MRI is less than 10 minutes, possibly allowing for a more cost-effective screening liver MRI than our cMRIs.

REFERENCES

1. Stewart BW, Wild C. World cancer report 2014. Lyon, France, Geneva, Switzerland: International Agency for Research on Cancer 2014.

2. Andersson KL, Salomon JA, Goldie SJ, Chung RT. Cost effectiveness of alternative surveillance strategies for hepatocellular carcinoma in patients with cirrhosis. *Clin Gastroenterol Hepatol*. 2008;6:1418–1424. [PubMed: 18848905]
3. Colli A, Fraquelli M, Casazza G, et al. Accuracy of Ultrasonography, Spiral CT, Magnetic Resonance, and Alpha-Fetoprotein in Diagnosing Hepatocellular Carcinoma: A Systematic Review. CME. *The American Journal of Gastroenterology*. 2006;101:513–523. [PubMed: 16542288]
4. Bruix J, Sherman M, American Association for the Study of Liver Diseases. Management of hepatocellular carcinoma: an update. *Hepatology*. 2011 pp. 1020–1022.
5. Liver Imaging Reporting and Data System. www.acr.org. <https://www.acr.org/Quality-Safety/Resources/LI-RADS>. Accessed August 9, 2017.
6. Cruite I, Tang A, Sirlin CB. Imaging-based diagnostic systems for hepatocellular carcinoma. *American Journal of Roentgenology*. 2013;201:41–55. [PubMed: 23789657]
7. Rofsky NM, Lee VS, Laub G, et al. Abdominal MR imaging with a volumetric interpolated breath-hold examination. *Radiology*. 1999;212:876–884. [PubMed: 10478260]
8. Pietryga JA, Burke LMB, Marin D, Jaffe TA, Bashir MR. Respiratory motion artifact affecting hepatic arterial phase imaging with gadoxetate disodium: examination recovery with a multiple arterial phase acquisition. 2014;271:426–434.
9. Rosset A, Spadola L, Ratib O. Osiri X: An Open-Source Software for Navigating in Multidimensional DICOM Images. *J Digit Imaging*. 2004;17:205–216. [PubMed: 15534753]
10. Landis JR, Koch GG. An application of hierarchical kappa-type statistics in the assessment of majority agreement among multiple observers. *Biometrics*. 1977;33:363–374. [PubMed: 884196]
11. Lee YJ, Lee JM, Lee JS, et al. Hepatocellular Carcinoma: Diagnostic Performance of Multidetector CT and MR Imaging-A Systematic Review and Meta-Analysis. 2015;:140690.
12. Ikram NS, Yee J, Weinstein S, et al. Multiple arterial phase MRI of arterial hypervascular hepatic lesions: improved arterial phase capture and lesion enhancement. *Abdominal Radiology*. 2017;42:870–876. [PubMed: 27770162]
13. Kee K-M, Lu S-N. Diagnostic efficacy of ultrasound in hepatocellular carcinoma diagnosis. *Expert Rev Gastroenterol Hepatol*. 2017;11:277–279. [PubMed: 28162003]
14. Ehman EC, Behr SC, Umetsu SE, et al. Rate of observation and inter-observer agreement for LI-RADS major features at CT and MRI in 184 pathology proven hepatocellular carcinomas. *Abdominal Radiology*. Springer US. 2016;41:963–969.
15. Davenport MS, Khalatbari S, Liu PSC, et al. Repeatability of diagnostic features and scoring systems for hepatocellular carcinoma by using MR imaging. 2014;272:132–142.

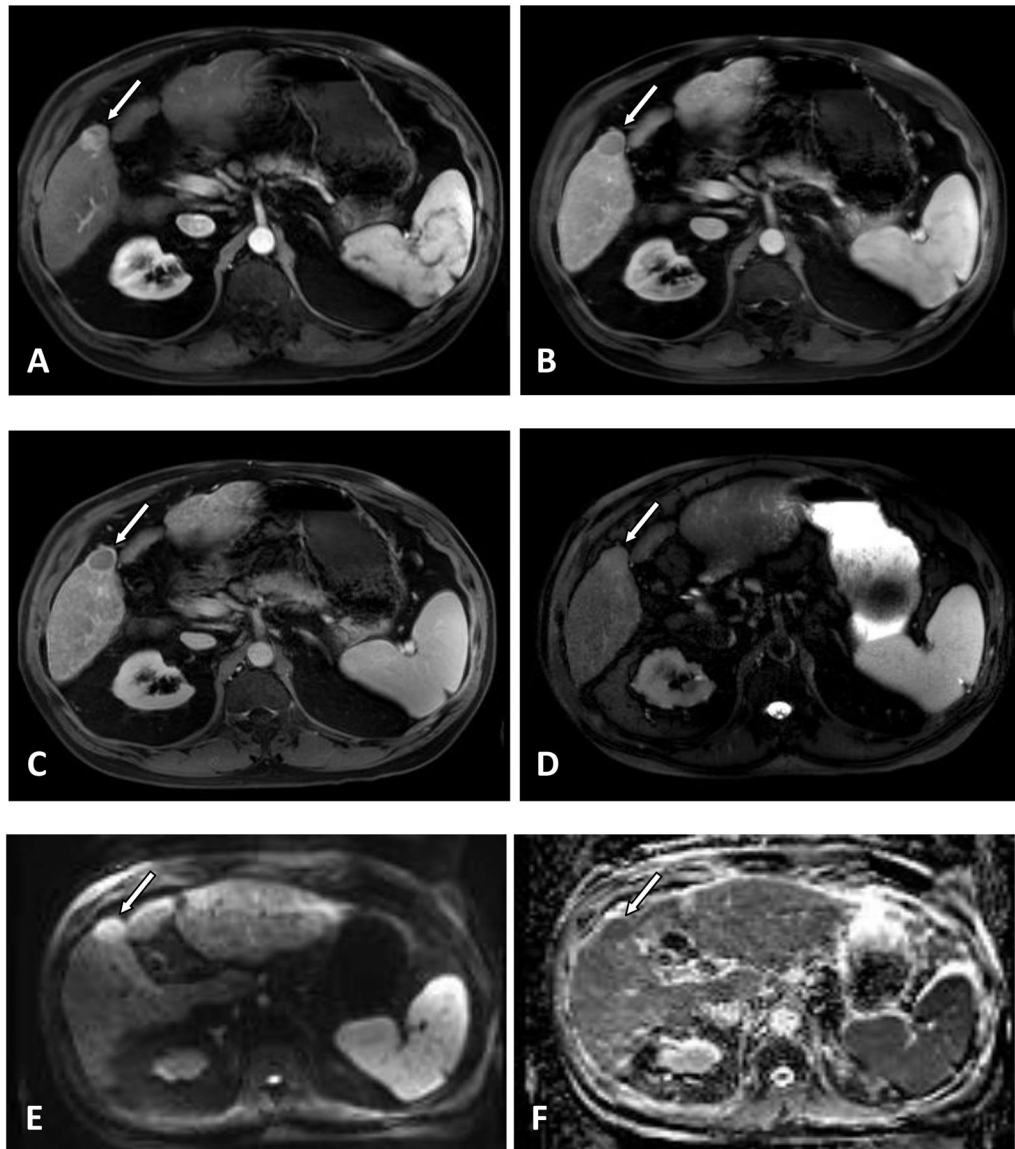


Figure 1: 65-year-old male with hepatitis C and elevated AFP with a 2.7 cm arterially enhancing lesion in segment 5 (A, arrow) with washout (B, arrow) and capsule (C, arrow), meeting LI-RADS 5 criteria. Ancillary features including faint T2 hyperintensity (D, arrow) and moderate diffusion restriction, as evidenced by hyperintensity on the high-B-value diffusion-weighted images (E, arrow) with low value on the corresponding ADC map (F), which did not affect the LI-RADS categorization.

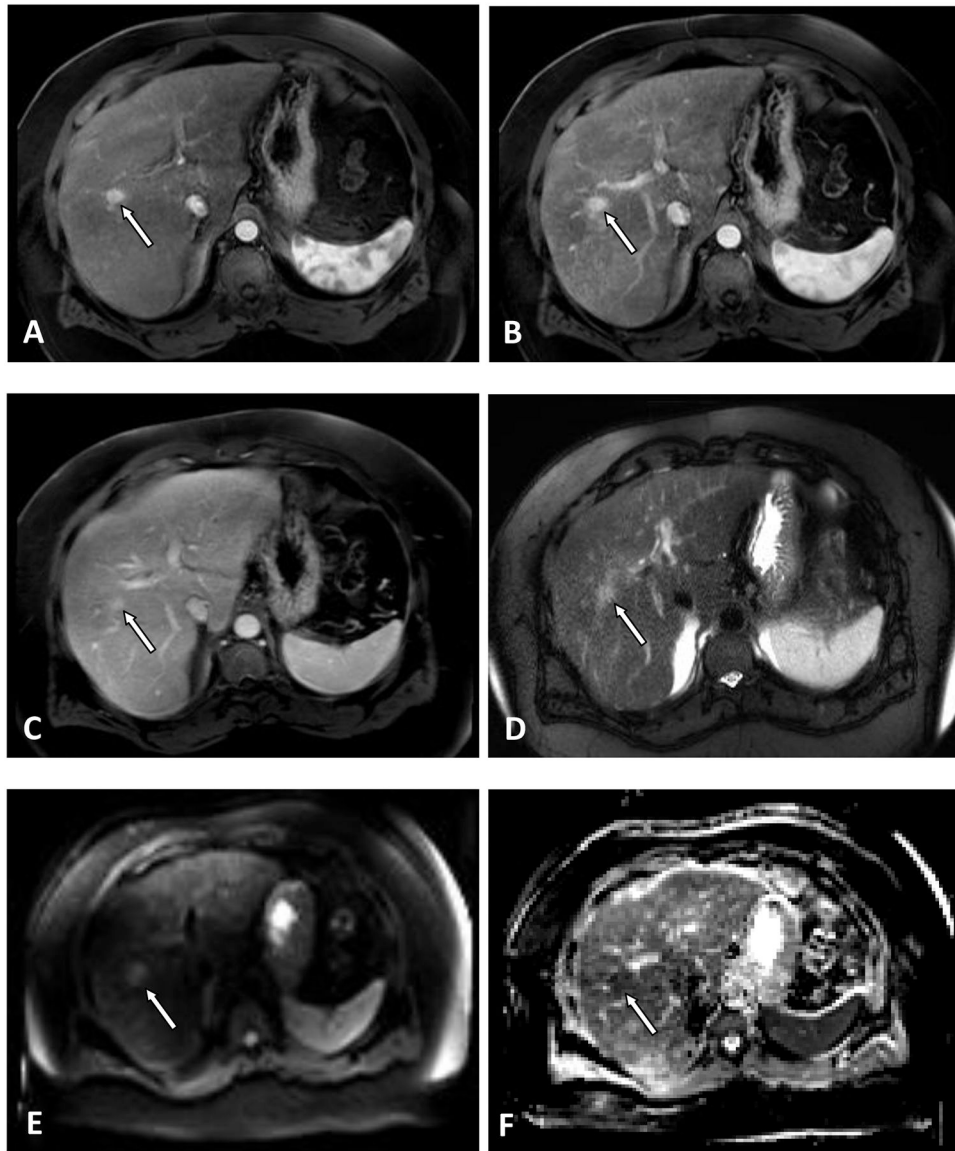


Figure 2: 65-year-old male with history of hepatitis C and alcohol abuse with a 1.5 cm lesion in the mid right hepatic lobe (arrow) that demonstrates arterial phase hyperenhancement (A and B, arrow) without evidence of washout (C, arrow), which would be categorized as LI-RADS 3 on an abbreviated protocol (aMRI). However, the presence of T2 hyperintensity (D, arrow) and mild diffusion restriction (E and F, arrow) upgrades the lesion to LI-RADS 4 on cMRI.

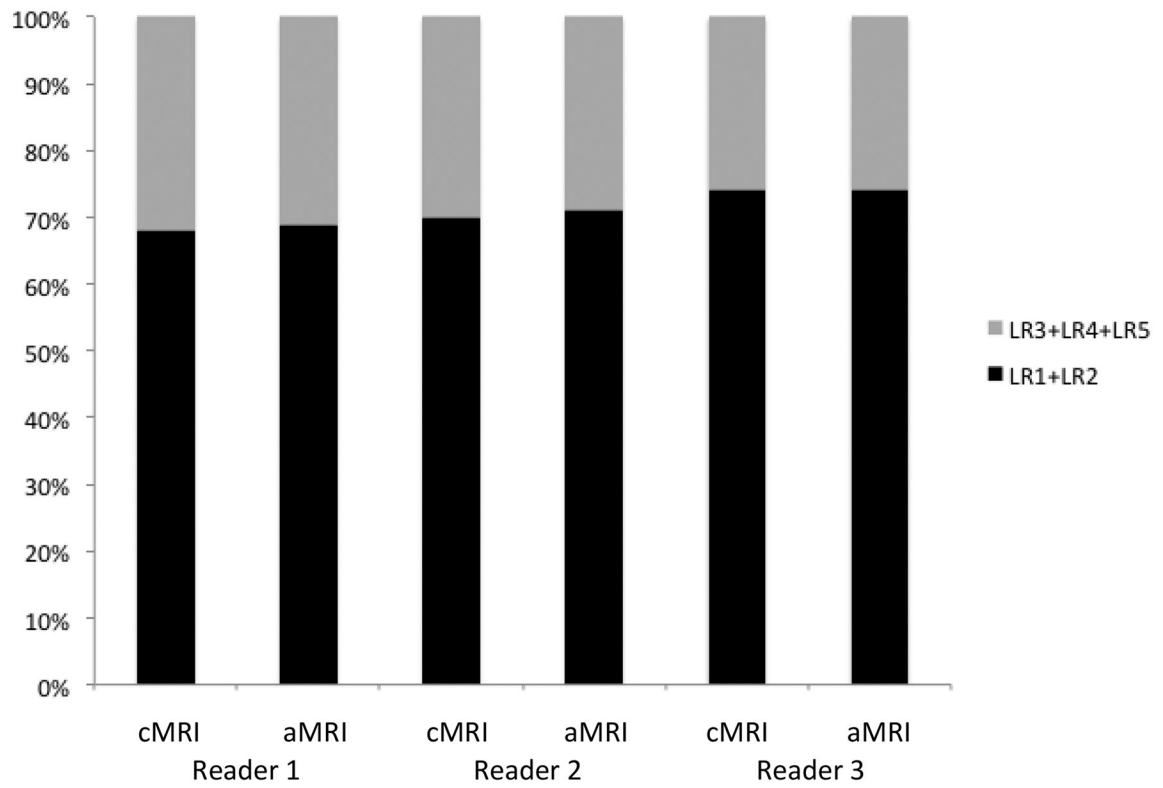


Figure 3:

Breakdown by reader of percent of studies categorized as either LI-RADS 1 and LI-RADS 2 combined (black) are compared with LI-RADS 3, 4 and 5 combined (light gray), demonstrating strong agreement between aMRI and cMRI for all three readers (kappa = 0.51 and 0.49 for aMRI and cMRI, respectively).

Table 1:

Demographic information for 164 patients who underwent screening liver MRI for HCC. Cirrhosis was documented based on either percutaneous biopsy or imaging results. Patients with known HCC or history of HCC treated with embolization therapy were not included.

age:	range 50–85 mean 64, standard deviation 6
gender:	5 female (3%), 159 male (97%)
etiology of liver disease:	118 hepatitis C (72%) 17 hepatitis B (10%) 32 alcohol (20%) 3 other (NAFLD, etc.) (2%)
cirrhosis:	131 (80%)
history of HCC:	38 (23%)

Author Manuscript

Author Manuscript

Author Manuscript

Author Manuscript

Table 2:

LI-RADS scores based on the highest LI-RADS categorized lesion/observation in each patient for each of the three readers using the abbreviated MRI (aMRI) and the complete MRI (cMRI).

	Reader 1		Reader 2		Reader 3	
	cMRI	aMRI	cMRI	aMRI	cMRI	aMRI
LI-RADS 1:	74 (47%)	76 (49%)	96 (62%)	96 (61%)	93 (60%)	93 (60%)
LI-RADS 2:	32 (21%)	32 (20%)	13 (8%)	15 (10%)	22 (14%)	22 (14%)
LI-RADS 3:	23 (15%)	29 (19%)	20 (13%)	23 (15%)	18 (11%)	19 (12%)
LI-RADS 4:	19 (12%)	11 (7%)	17 (11%)	13 (8%)	9 (6%)	8 (5%)
LI-RADS 5:	8 (5%)	8 (5%)	10 (6%)	9 (6%)	14 (9%)	14 (9%)

Author Manuscript

Author Manuscript

Author Manuscript

Author Manuscript

Table 3:

Inter-reader agreement (kappa) among the three readers for LI-RADS scores and major features for highest LI-RADS categorized lesion in 156 subjects for the abbreviated MRI (aMRI) and the complete MRI (cMRI).

	Reader 1	Reader 2	Reader 3	Agreement (κ)
aMRI: LI-RADS 1/2	108	111	115	
LI-RADS 3	29	23	19	
LI-RADS 4	11	13	8	0.305
LI-RADS 5	8	9	14	
aMRI: LR1/LR2	108	111	115	
LR3/LR4/LR5	48	45	41	0.508
cMRI: LI-RADS 1/2	106	109	115	
LI-RADS 3	23	20	18	
LI-RADS 4	19	17	9	0.308
LI-RADS 5	8	10	14	
cMRI: LR1/LR2	106	109	115	
LR3/LR4/LR5	50	47	41	0.489
imaging features:				
arterial hyperenhancement	72	63	52	0.354
washout appearance	15	23	18	0.355
capsule appearance	14	5	15	0.416